Solar Parabolic Dish Concentrator Field Performance Evaluation

John Fangman(✉), Sudhakar Neti, and Naoise Irwin

Solarflux Energy Technologies, Inc., 1017B MacArthur Road, Reading, PA 19605, USA
john.fangman@solarflux.co

Abstract. The field performance of the FOCUS, a near-parabolic dish concentrator developed by Solarflux Energy Technologies, Inc, (Solarflux) is reported. Parabolic dish concentrators are concentrating solar power (CSP) devices which focus Direct Normal Irradiance (DNI) on to a central receiver. The focused solar DNI is then collected as thermal energy which can be used to produce hot water or other fluid or steam for a variety of applications, including thermal uses and electricity generation. DNI was measured using a U.S. National Institute of Standards and Technology (NIST) referenced pyrheliometer attached to the FOCUS concentrator, and the data cross-referenced with other sources. Heat transfer fluid (HTF) temperature before and after the receiver was measured using thermocouples. The heat transfer fluid used was a 72/28 blend of DI water and propylene glycol. Flow rate was measured using a magnetic-induction digital flow meter. Where possible, sensor measurements were recorded and calculations were performed in accordance with American Society for Testing and Materials (ASTM) standards. The system response time was measured at 1 min 15 s, and the heat gain was calculated to be 72 W per 100 W/m^2 DNI, or 72%.

1 Introduction

The original impetus for the development of the FOCUS concentrator was a desire to find a viable sustainable energy solution for low-income rural populations in developing countries. According to the World Health Organization, around three billion people cook using polluting open fires or simple stoves fueled by kerosene, biomass (wood, animal dung and crop waste) and coal, and every year close to four million people die prematurely from illness attributable to household air pollution from inefficient cooking practices using polluting stoves paired with solid fuels and kerosene [1]. Furthermore, the unsustainable harvesting of fuel wood is major driver of forest degradation, adversely impacting more than 30 million hectares of forests in India alone [2]. In an effort to find a sustainable, low-cost, and resilient solution to this urgent problem, a thorough evaluation of available technologies was conducted.

A near-parabolic dish concentrator design was ultimately selected for ease of installation, flexible deployment capability, high efficiency, and potential for local manufacture and maintenance. Parabolic dish concentrators are acknowledged to be the most efficient CSP technology, in terms of both energy conversion and land-use. Historically, parabolic dish concentrators have been perceived as challenging to manufacture, due to the complex curvature of the dish as well as the additional moving parts required for two-axis

A. K. Ghosh and C. Rixham (Eds.): ASES SOLAR 2022, SPE, pp. 55–70, 2022.
https://doi.org/10.1007/978-3-031-08786-8_6

vs. single-axis tracking. However, the approach adoption by Solarflux has been to focus heavily on the performance vs. cost tradeoff in all design decisions, and to utilize proven volume manufacturing methods and commercially available components to maximize reliability and minimize unit costs. The result is the FOCUS, a general-purpose parabolic dish concentrator suitable for a wide range of applications.

Several advanced prototypes of the FOCUS were installed at Penn State University's Berks Campus (PSU Berks) in Reading, Pennsylvania, USA, during 2016, as part of a solar energy related investment program funded by the Commonwealth of Pennsylvania. The FOCUS units installed included one smaller unit with 13.9 m^2 of reflective aperture, as well as three larger units, each with 42.4 m^2 of reflective aperture. The smaller FOCUS unit was devoted to providing heat to a greenhouse operated by the agriculture center at Penn State Berks, while the larger units were devoted to concentrated photovoltaic (CPV) research. The focus of this paper is on the field performance data from the smaller FOCUS unit (PSU Berks unit). Annual estimated DNI for this location in Pennsylvania is in the range 2.82–4.91 kWh/m^2/day.

In this work we test the performance of the FOCUS in two key areas, conforming closely to the ASTM E905-87 standard. According to ASTM E905-87, there are two tests to be performed by the manufacturer of a two-axis point concentrator: (1) Response Time and (2) Heat Gain. Response time is measured to establish the time required to achieve quasi-steady state conditions before and during each thermal performance test to assure valid test data. Heat gain (Q) is the product of the HTF mass flow rate (m), its specific heat (C_p), and the temperature difference between the input and output of the receiver (t_a).

There are many practical factors that contribute to the final heat gain product, with major contributors being reflectivity of the mirror, intercept factor, and overall efficiency of the absorber. Based on the index of refraction and extinction coefficient, the ideal first surface aluminum reflector would have an average reflectivity of 93%. Best geometric optics will predict an intercept factor of 99%, and based on a typical heat exchanger, the receiver will have a 90% heat transfer efficiency. Multiplying these factors predicts an 83% total solar-to-heat efficiency, representing the theoretical maximum heat gain achievable by the FOCUS.

Once heat gain is determined experimentally, $R(\Theta)$, the ratio of the rate of heat gain to the solar power incident on the aperture of the collector can be calculated. The experimental results will be compared to the theoretical maximum, any deviation will be discussed and possible improvements will be identified.

2 Concentrator Description

The FOCUS consists of five major sub-components, common to all parabolic dish concentrators. These are the collector, the receiver, the tracker assembly, the controller, and the mast. The mast is mounted on the ground or on a rooftop. The tracker assembly is then placed on the mast, and the collector is placed on top of the tracker assembly. The receiver is positioned on the optic axis at the waist point of the collector. The controller manages the tracker assembly to determine the orientation of the collector, ensuring its optimal positioning relative to the sun.

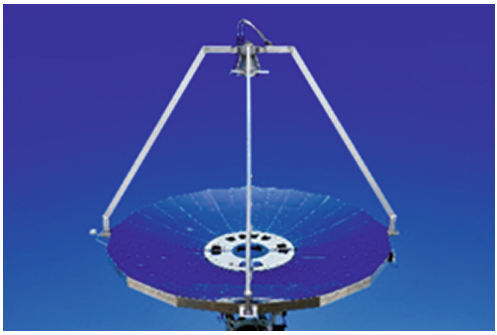

Fig. 1. FOCUS collector

The collector is made up of sixteen truncated sectors of a circle, forming petals. The petals are highly polished first surface aluminum mirrors consisting of 0.5 mm 1090 aluminum clad to a 1.5 mm, 3003 structural aluminum substrate. Each petal is self-supporting, not requiring a separate structure to either maintain mirror alignment to the optic axis, or provide the structural strength required for wind events. The petals have mechanical alignment features to ensure proper alignment to adjacent petals. Once attached to each other the petals form a self-supporting parabolic dish collector. Figure 1 shows the collector and receiver. The collector geometry is a segment of a spindle toroid. In the above configuration it has a total clear aperture of 13.94 m^2 and delivers a geometric concentration ratio greater than 2,000, verified using Zemax modeling. The collector's design is further described in the US patent 8680391, which covers several of the key features of the FOCUS.

Fig. 2. Thermal receiver

The FOCUS collector demonstrates total solar weighted hemispherical reflectance of 89.6% [3]. The FOCUS collector's specular reflectance (the portion of the solar spectrum directed at the focal plane), a surface reflectance property, is measured at 85.6% [4]. Integrating the specular reflectance with ASTM G173–03, a reference for the terrestrial spectral distribution of solar irradiance, predicts an 83.8% solar-weighted specular reflectance for the collector. Prior to the installation of the collector at PSU Berks in 2016 the specular reflectance of the collector's surface aluminum averaged 84.1%, in the 400 nm and 1050 nm wavelength range [5]. In March 2021, the aluminum surface was cleaned for the first time since installation. Reflectance testing was then repeated over the same wavelengths and

using the same instrument, with average specular reflectance measured at 83.5%. Comparing this measurement against the identical test performed on the same aluminum prior to installation five years earlier, we observe a modest 0.6% loss of specular reflectance after exposure to dust, birds, insects, aerosols and other atmospheric effects.

The thermal cavity receiver (see Fig. 2) is compact and light weight (~52 lbs/23.6 kg). It consists of four components: the absorber, housing, insulation, and a heat shield. The absorber is a trucated cone with a 300 mm diameter aperture that tapers down to 140 mm diameter and is 360 mm deep. It is fabricated using 0.5 in. diameter 0.035 wall thick copper tubing. The absorber is coated with a black body ceramic coating, with a 593 °C operating temperature, and emissivity greater than 0.9. The absorber is housed in an aluminum casting, with a 12 mm layer of ceramic insulation between the coil and the receiver housing. The heat shield is polished stainless steel and mounted at the entrance pupil of the receiver, protecting the aluminum housing from concentrated radiation.

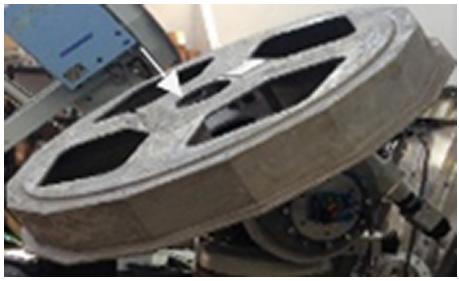

Fig. 3. Tracker assembly

The tracker assembly, shown in Fig. 3, is arranged in an azimuth and zenith configuration. It consists of a cast hub, slew drives, gearboxes, motors, encoders, and a controller. The azimuth has a range of motion of 360°, the Zenith 90°. The slew drives at each axis are hourglass worm drives that have a gear ratio of 85:1, with a precision of $\leq$0.09° and efficiency of 40%. Coupled to the input of the slew drive is a planetary gear box with a 256:1 gear ratio and efficiency of 89%. Drive power to each axis is supplied by a 400 step per revolution stepping motor. All components used in the assembly of the tracker are IP65 rated, providing robust environmental resilience. The assembled collector is slid onto the hub (like a split rim of a truck wheel). A retaining ring secures the collector to the hub while allowing it to freely expand and contract. The hub is connected to the slew drives by two custom castings.

Tracking control of the FOCUS concentrator is a hybrid between active feedback and open loop control. An optical sensor module is mounted on the collector and provides $\pm$0.05° feedback to the tracking controller. Additionally, encoders with a resolution of $\pm$0.01° are mounted on each axis to measure the true azimuth and zenith angles. At the beginning of each day and after the optical sensor module locks on to the sun the encoders are calibrated by comparing their readings to the National Renewable Energy Laboratory (NREL) solar position algorithm. During clear sky conditions active feedback from the optical module is used for tracking feedback, while broken skies and other weather events require the use of the encoders. The other function of the dish controller is safety and monitoring. Wet bulb thermocouples are attached to the input and output of the thermal receiver. If the temperature of the HTF exceeds preset limits, the controller will move the dish out of the sun. If the wind exceeds 30 mph (48 kph) the dish is moved into the wind safe position with the receiver pointing vertically up at the sky. Tracking is resumed

once the wind has subsided. Failure mode analysis and field experience suggests that the FOCUS can withstand winds of at least 90 mph (144 kph) in safe mode.

The FOCUS concentrator is mounted on an 11 foot long mast consisting of sixteen-inch diameter galvanized Sch. 40 pipe, with a companion flange at each end. One end of the mast is bolted to the concrete foundation with the tracking mechanism bolted to the other.

3 Test Site and Instrumentation Overview

The PSU Berks unit was installed at Penn State University's Berks Campus. The concentrator is utilized to supply thermal energy to a greenhouse operated by the agriculture department at Penn State Berks. The GPS location of the PSU Berks FOCUS concentrator are 40° 21′ 51″ N and 75° 58′ 34″ W, with an elevation of 73 m [6]. Figure 4 shows the concentrator in the center of the image and the greenhouse to the East side. A utility shed (not shown) was subsequently built to the southeast of the greenhouse to host thermal loop related equipment.

Fig. 4. PSU Berks FOCUS concentrator installation location

Fig. 5. PSU Berks FOCUS concentrator

The PSU Berks FOCUS concentrator is shown in Fig. 5.

Figure 6 below provides an illustration of the system components, including placement of the thermocouples, at the Penn State Berks test site.

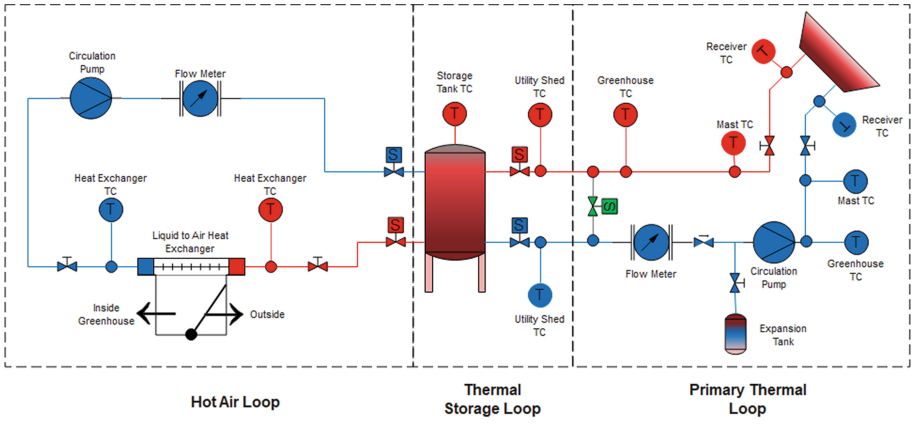

Fig. 6. PSU Berks FOCUS greenhouse system thermocouple placement

The system in Fig. 6 is divided into three thermal loops. At the beginning of each day HTF is circulated through the primary thermal loop. HTF is circulated from the receiver output to the greenhouse where it is diverted back to the input of the thermal receiver. This continues until the temperature of the HTF from the receiver exceeds that of the storage tank. Once the target temperature is achieved, a diverter valve opens to let the HTF circulate through the thermal storage loop and back out to the thermal receiver. This circulation continues until the storage tank reaches its maximum storage temperature or

the greenhouse requires heat. When these conditions are met the hot air loop is opened, which circulates the HTF between the storage tank and the liquid to air heat exchanger. For the purposes of these tests all three thermal loops were manually opened, which dissipated heat produced by the collector and maintained the input temperature to the collector.

The instrumentation used is described in Table 1 below.

Table 1. Instrumentation

Instrument	Description	Image
Pyrheliometer (DNI Sensor)	• EKO, model no.: MS-57 • Field of view 5° • WRR scale • Operating temperature range: -40 - 80□ • Solar spectral range: 200 – 4000 nm • Solar irradiance range 0-1600 W/m^2 • Calibrated results: 8.297 µV/W*m^2 sensitivity with 0.36% uncertainty • Response time: 99% after 6 sec	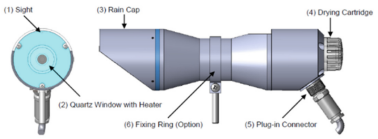
A-Box-I Signal converter	• Analogue interface (V) • 4-20 mA | 0-1600 W/m2 Irradiance • Correction for sensor temperature dependency and non-linearity • IP65 All-weather enclosure • Optional USB controller and EKO sense control software • Ingress protection: 65	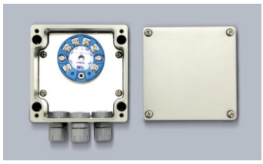
Weather station	• Davis model 6163 • Data updates every 2.5 seconds. • Outside temperature ±0.3°and humidity sensors ±2% • Wind speed ±5%, and direction ±3° • Rainfall • UV and GHI Solar radiation ±5% full scale, and range 0-1800w/m²	
Magnetic-inductive flow meter	• IFM • Model SM7604 • Measuring range: 0.2-50 l/min • Resolution: 0.1 l/min • Flow monitoring accuracy: ± (2% MW + 0.5% MEW) • Response time: 0.15 s	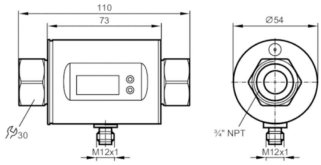
Circulation pump	• Model: UPS 26-150 SF • Maximum flow: 11.81 m³/h • Pumped liquid: water/glycol • Liquid temperature range: 0 - 110 °C	
Optical sensor module	• FusioSeeker • Model DS-50-D6W • Accuracy ± 0.05°	
Absolute axis encoder	• Baumer • Model: GBA2W • Absolute accuracy ±0.01° • Single turn • 524288 / 19 bit steps per revolution	
Thermalcouple	• Type K thermal couple from Omega	

4 Test Setup

Pursuant to the ASTM E905-87 standard, we evaluated the performance of the FOCUS in the two key areas where testing is required for a two-axis point concentrator: (1) Response Time and (2) Heat Gain. Each test is considered in turn.

For the Response Time test, the following preparatory steps were taken prior to testing. The FOCUS collector was cleaned using 'Simple Green' all-purpose cleaner diluted 10:1 with filtered spring water. A microfiber cloth was then used to gently scrub the surface of the dish. A high-pressure washer (1,700 psi) used to rinse dish after cleaning, using filtered spring water. The DNI sensor lens was cleaned using clean dry microfiber cloth, and alignment with sun verified. The propylene glycol HTF concentration was measured using an ATC refractometer at 28% propylene glycol in 72% DI water. Circulation pumps were activated manually, all loops were opened and the heat exchanger blower was turned on one hour before testing to stabilize HTF input temperature at the receiver.

Mass balance for the HTF before and after the FOCUS concentrator was met, where the liquid mass flow entering the concentrator is the same as the liquid mass flow leaving the concentrator at any specific time. The HTF mass flow rate is calculated based on the instantaneous flow rate obtained by the magnetic-inductive flow meter and the heat transfer fluid density at the arithmetic mean temperature of the inlet and outlet of the FOCUS receiver. The flow meter measuring range is 0.2 to 50 L/m, while the maximum flow rate of the heat transfer fluid observed is around 8 L/m. Figure 7 shows the correlation between the heat transfer fluid density and its temperature.

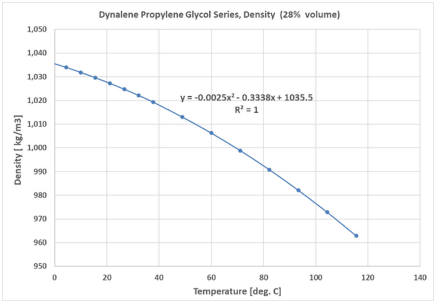

Fig. 7. Heat transfer fluid density vs. temperature

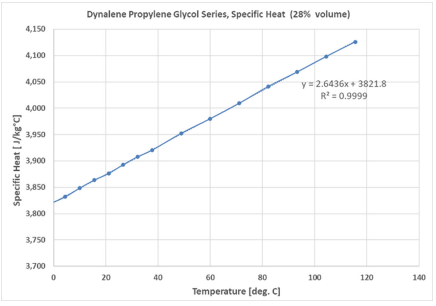

Fig. 8. Heat transfer fluid specific heat vs. temperature

For the area of interest, which is the heat transfer fluid between the FOCUS concentrator's receiver inlet and outlet, the energy balance for the heat transfer fluid will neglect the potential and kinetic energies. Also, it was assumed that no external work has been applied to the heat transfer fluid, and no phase change occurred. Thus, the energy collected through the FOCUS concentrator will be transferred to the heat transfer fluid, minus any losses. The rate of heat/enthalpy gain (Q) is calculated from its defining relationship:

$$Q = \left(mC_p\right)\Delta t_a \tag{1}$$

where the product of mass flow rate and specific heat (mC_p) are determined using the plots shown in Figs. 7, and 8, at the mean value of inlet and outlet temperatures of the receiver, and (Δt_a) is the difference between the inlet temperature (t_{fi}) and output temperatures (t_{fe}) of the receiver

$$\Delta t_a = t_{fe} - t_{fi} \tag{2}$$

Conversion rate $R(\Theta)$ = the rate of heat gain (Q) divided by the product of the direct solar irradiance (DNI, $E_{s,DN}$) and the collector aperture (A_a) becomes:

$$R_\Theta = Q/E_{s,DN}A_a \tag{3}$$

5 Response Time Test Performance and Results

The response time test was conducted by Solarflux personnel led by Solarflux Chief Technology Officer and Principal Engineer John Fangman, in accordance with the guidelines outlined in ASTM E905-87, Sect. 21.1, and Procedure B. The test was conducted on June 6th, 2021.

At 11:10:57am the FOCUS collector was moved from its maintenance position to an azimuth angle of 116.41°, and zenith to 22.5°, as compared to the suns position at azimuth 118.39, and zenith 28.41. The collector remained in this position until the start of the test. The data shown in Table 2 were recorded every 15 seconds during the waiting period to establish steady state prior to the beginning of the test. The inlet temperature ($t_{f,I}$) varied ±0.2 °C, compared to maximum ±0.2 °C required for steady state. The temperature

Table 2. Data recorded during wait time prior to response time test

Parameter	Symbol	Average	Maximum	Minimum	±Range
Temperature of the HTF at the inlet of the Receiver	$t_{f,I}$	34.2	34.4	33.9	0.25
Mass flow of HTF	m	0.135	0.136	0.134	0.001
Energy associated with sensible heat of HTF	(mC_p)	0.524	0.527	0.521	0.003
Direct normal irradiance projected onto the collector	$E_{s,D}$	0.000	0.000	0.000	0.000
Global horizontal irradiance	$E_{s,2\pi}$	808.750	810.000	805.000	2.50
Temperature difference of HTF between receiver input and output	Δt_a	0.020	0.200	-0.100	0.15
Ambient air temperature	t_{amb}	29.919	30.000	29.778	0.11
Wind speed	m/sec	0.872	2.235	0.000	1.12

difference between the input and output (Δt_a) varied by ±0.1 °C compared to maximum ±0.4 °C required for steady state. Measured (mC_p) varied ±0.6% compared to maximum ±1.0% required for steady state. Direct irradiance ($E_{s,DN}$) measured at this position was 0.0 W/m^2 with 0.0% variation. Global irradiance ($Es,_{2\pi}$) varied ±0.3% compared to maximum ±4% required for steady state. Ambient temperature (t_{amb}) varied ±0.1 °C compared to maximum ±2.0 °C required for steady state. Maximum wind speed was 2.35 m/s compared to <4.5 m/s maximum for steady state.

At 11:16:57am the collector was placed in tracking mode, moving the collector from its waiting position to the collector aperture normal to the sun. At 11:17:42 the collector aperture completed its motion and aligned normal to the sun. At 11:23:42 the response time test was completed. Data were recorded every 15 s for the duration of the test, and plotted in Fig. 9.

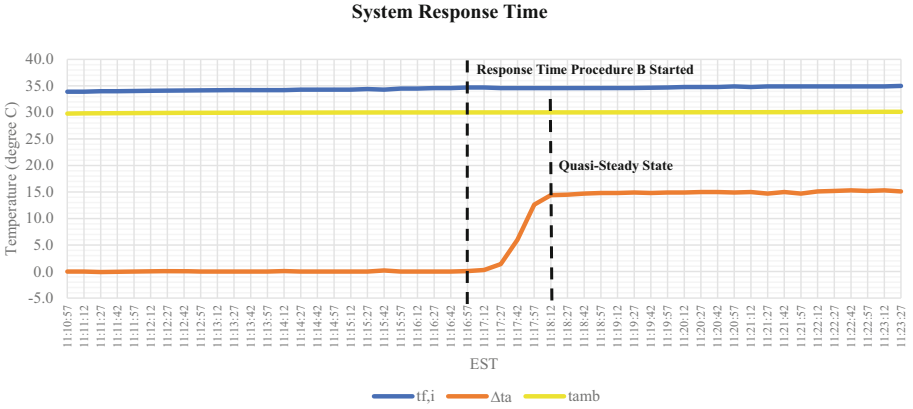

Fig. 9. Response time plot

In accordance with ASTM E905-87 Procedure B quasi-steady state is achieved when the equation below is satisfied:

$$\left(\Delta t_{a,f} - \Delta t_{a,T}\right)/\left(\Delta t_{a,f} - \Delta t_{a,i}\right) = 0.10 \tag{4}$$

where:

$\Delta t_{a,f}$ is the temperature difference across the receiver inlet and outlet at final quasi-steady state condition
$\Delta t_{a,i}$ is the temperature difference across the receiver inlet and outlet at the initial start condition
$\Delta t_{a,T}$ is the temperature difference across the receiver inlet and outlet at the start of the quasi-steady state condition.

Substituting measurements taken during testing, $\Delta t_{a,f} = 15.10$, and $\Delta t_{a,i} = 0.08$, and solving for ($\Delta t_{a,T}$), quasi-steady state is achieved when the temperature difference across the receiver reaches 13.59 °C. This was achieved at 11:18:12am. Compared to

the start time of the test (11:16:57am), the response time is determined to be (1 m 15 s) one minute fifteen seconds.

A summary of the data between the onset of quasi-steady state and the completion of the test is shown in Table 3. The inlet temperature ($t_{f,I}$) varied ±0.2 °C, compared to maximum ±0.2 °C required for steady state. The temperature difference between the input and output (Δta) varied by ±0.3 °C compared to maximum ±0.4 °C required for steady state. Measured (mC_p) varied ±1.3% compared to maximum ± 1.0% required for steady state. Fluctuations in the circulation pump flow rate was the contributor to this variation, and appears to be in the normal range of this pump. Direct irradiance ($E_{s,DN)}$ averaged 839.7 w/m^2 ±0.25%, compared to a maximum allowed variation of ±4%. Global irradiance ($Es,_{2\pi}$) varied ±0.3% compared to maximum ±4% required for steady state. Ambient temperature (t_{amb}) varied ±0.11 °C compared to maximum ±2.0 °C required for steady state. Maximum wind speed was 1.34m/sec compared to <4.5 m/s maximum for steady state.

Table 3. Taken over 5-min period after achieving steady state

Parameter	Symbol	Average	Maximum	Minimum	±Range
Temperature of the HTF at the inlet of the Receiver	$t_{f,I}$	34.8	35.0	34.6	0.20
Mass flow of HTF	m	0.135	0.137	0.133	0.00
Energy associated with sensible heat of HTF	(mC_p)	0.531	0.539	0.524	0.01
Direct normal irradiance projected onto the collector	$E_{s,D}$	839.638	842.022	837.138	2.44
Global horizontal irradiance	$Es,2\pi$	819.619	824.000	817.000	3.50
Temperature difference of HTF between receiver input and output	Δt_a	14.971	15.300	14.700	0.30
Ambient air temperature	t_{amb}	30.045	30.111	30.000	0.06
Wind speed	m/sec	0.596	1.341	0.000	0.67

6 Rate of Heat Gain Test

The test procedure for "Rate of Heat Gain at Near Normal Incidence" is described in Sect. 13.5 of the ASTM E905-87 standard. The application of the PSU Berks concentrator is to provide space heating to the PSU Berks greenhouse. As such, the temperature is never to exceed 100 °C, which limits the range of input temperatures that can be evaluated. It is difficult to produce four equally spaced values of input temperatures, as specified in Sect. 13.5 for an application with such a narrow range. As such heat gain

was evaluated at 42 °C, 52 °C, 66 °C, and 72 °C. The data sets used for this evaluation are consistent with the quasi-steady state condition, which for this system is one minute fifteen seconds. Also, per Sect. 10.1 of the ASTM the condition must exist for a period equal to two times the response time. Once these criteria are met the data may be used to calculate the rate of heat gain (Q) using Eqs. (1), and (2).

Values for mass flow (m), and specific heat (Cp) were determined by using the mean temperature between the input and output of the receiver (Δt_a) for each test and the expressions shown in Figs. 7 and 8. All heat gain tests were conducted on June 6th, 2021 between the hours of 11:30am to 4:47pm.

Table 4 is the summary data to validate that a quasi-steady state condition existed during the 42 °C inlet temperature testing. The data were taken over a five-minute period starting at 11:31am. Substituting values from Table 4 into Eq. (1) for calculating heat gain, average Q = 8.28 kW ± 0.07 kW. Further, substituting the value for Q into Eq. (3) where:

$E_{s,D}$ = direct normal incidence (w/m^2) on the collector from Table 3

A_a = the clear aperture of the collector, which is 13.94 m^2.

The ratio of the rate of heat gain (Q) to the solar power incident on the aperture can be calculated (R_Θ):

$$R_\Theta = 0.70, \text{ or } 70.0\% \text{ solar-to-thermal conversion}$$

Table 4. Quasi-steady state summary data 42 °C Inlet

Parameter	Symbol	Average	Maximum	Minimum	±Range
Temperature of the HTF at the inlet of the Receiver	$t_{r,I}$	34.6	42.4	0.0	21.20
Mass flow of HTF	m	3.217	3.932	0.000	1.97
Energy associated with sensible heat of HTF	(mC_P)	6.487	8.360	0.008	4.18
Direct normal irradiance projected onto the collector	$E_{s,D}$	549.854	852.399	0.005	426.20
Global horizontal irradiance	$Es,2\pi$	691.212	846.000	0.002	423.00
Temperature difference of HTF between receiver input and output	Δt_a	12.679	15.600	0.006	7.80
Ambient air temperature	t_{amb}	27.346	30.444	0.056	15.19
Wind speed	m/sec	1.679	3.129	0.155	1.49

Table 5 is the summary data to validate quasi-steady state condition existed during 52 °C inlet temperature testing. The data was taken over a five-minute period starting at 12:38pm. Substituting values from Table 5 into Eq. (1) for calculating heat gain, average

Q = 8.49 kW ± 0.07 kW. Further, substituting the value for Q into Eq. (3), the ratio of the rate of heat gain (Q) to the solar power incident on the aperture (R_Θ) is calculated:

$$R_\Theta = 0.71, \text{ or } 71.0\% \text{ solar-to-thermal conversion}$$

Table 5. Quasi-steady state summary data 52 °C Inlet

Receiver Input Temperature 52°C					
Parameter	Symbol	Average	Maximum	Minimum	±Range
Temperature of the HTF at the inlet of the Receiver	$t_{f,I}$	52.6	52.7	52.3	0.20
Mass flow of HTF	m	0.113	0.114	0.113	0.001
Energy associated with sensible heat of HTF	(mC_p)	0.448	0.452	0.446	0.003
Direct normal irradiance projected onto the collector	$E_{s,D}$	855.676	858.808	852.399	3.20
Global horizontal irradiance	$Es,2\pi$	904.474	911.000	902.000	4.50
Temperature difference of HTF between receiver input and output	Δt_a	18.937	19.100	18.800	0.15
Ambient air temperature	t_{amb}	31.576	31.611	31.500	0.06
Wind speed	m/sec	2.682	2.682	2.682	0.00

Table 6 is the summary data to validate quasi-steady state condition existed during 66 °C inlet temperature testing. The data was taken over a five-minute period starting at 3:16pm. Substituting values from Table 6 into Eq. (1) for calculating heat gain, average Q = 7.59 kW ± 0.16 kW. Further, substituting the value for Q into Eq. (3), the ratio of the rate of heat gain (Q) to the solar power incident on the aperture can be calculated (R_Θ).

$$R_\Theta = 0.72, \text{ or } 72.0\% \text{ solar-to-thermal conversion}$$

Table 7 is the summary data to validate quasi-steady state condition existed during 72 °C inlet temperature testing. The data was taken over a five-minute period starting at 4:41pm. Substituting values from Table 7 into Eq. (1) for calculating heat gain, average Q = 7.04 kW ± 0.16 kW. Further, substituting the value for Q into Eq. (3), the ratio of the rate of heat gain (Q) to the solar power incident on the aperture can be calculated (R_Θ).

$$R_\Theta = 0.72, \text{ or } 72.0\% \text{ solar-to-thermal conversion}$$

Table 6. Quasi-steady state summary data 66 °C Inlet

Receiver Input Temperature 66°C					
Parameter	Symbol	Average	Maximum	Minimum	±Range
Temperature of the HTF at the inlet of the Receiver	$t_{r,I}$	66.6	66.8	66.4	0.20
Mass flow of HTF	m	0.114	0.115	0.113	0.001
Energy associated with sensible heat of HTF	(mC_P)	0.457	0.459	0.453	0.003
Direct normal irradiance projected onto the collector	$E_{s,D}$	759.370	773.044	746.490	13.28
Global horizontal irradiance	$Es,2\pi$	793.700	803.000	788.000	7.50
Temperature difference of HTF between receiver input and output	Δt_a	16.635	17.000	16.300	0.35
Ambient air temperature	t_{amb}	32.608	32.611	32.556	0.03
Wind speed	m/sec	5.812	5.812	5.812	0.00

Table 7. Quasi-steady state summary data 72 °C Inlet

Receiver Input Temperature 72°C					
Parameter	Symbol	Average	Maximum	Minimum	±Range
Temperature of the HTF at the inlet of the Receiver	$t_{r,I}$	72.0	72.2	71.9	0.15
Mass flow of HTF	m	0.114	0.115	0.113	0.001
Energy associated with sensible heat of HTF	(mC_P)	0.458	0.461	0.454	0.004
Direct normal irradiance projected onto the collector	$E_{s,D}$	700.204	710.475	683.311	13.58
Global horizontal irradiance	$Es,2\pi$	617.130	624.000	601.000	11.50
Temperature difference of HTF between receiver input and output	Δt_a	15.365	15.600	15.100	0.25
Ambient air temperature	t_{amb}	32.937	32.944	32.889	0.03
Wind speed	m/sec	2.838	5.364	1.341	2.01

7 Test Results and Discussion

It should be noted that the FOCUS system used to conduct these tests is a developmental prototype intended to demonstrate the use of a Solarflux designed concentrator in a space heating application. Thus, other than the DNI sensor, all the instrumentation and hardware used such as the circulation pump, weather station, valves, storage tank etc., are typical of those used in any of our standard installations. The DNI sensor is a Class I device, as required by the ASTM standard. The DNI sensor is mounted on the receiver frame and not on its own independent tracker. Global solar irradiance measurements are also recorded by a Davis 6163 weather station located at the Penn State Berks site and measurements were verified to be consistent with historical DNI and GHI measurements taken from NREL, NASA, and NOAA databases at this location in early June.

The 'response time' is not a test but a characterization of the installed system. Only data recorded after the response time has elapsed can be considered valid results for subsequent tests. Since the tests were conducted on a two-axis tracking point concentrator, it had to be and was moved within a few degrees of tracking prior to the test. Subsequently, part of the response time includes the time required to move from the waiting position to optical alignment and tracking with the sun, and therefore the seventy-five second response of the system is a conservative measurement.

The heat gain tests were performed on the **same day, and immediately after the response time study**. Using quasi-steady state criteria, the enthalpy change (Q) as it relates to DNI and input temperature was ascertained. Substituting the value (Q) for each input temperature into the expression;

$$R_{\Theta} = Q/E_{s,DN}A_a,$$

where Q is the solar heat conversion, $E_{s,DN} * A_s$ is the incident solar power.

The peak ratio of heat gain to solar power incident on the aperture was calculated at 0.72, at input temperatures >66 °C.

Achieving the theoretical maximum of 83% solar-to-thermal conversion efficiency as discussed in the ideal concentrator model is not practically possible. The reflectance of the aluminum in the ideal model is an average over all wavelengths of light. All reflective surfaces have their own spectral response governed by their index of refraction and extinction coefficients. Aluminum has lower reflectivity in the shorter wavelengths and over 98% in wavelengths above the near infrared. Additionally, as is well known and documented in ASTM G173-03 energy distribution of solar irradiance varies by wavelength. Integrating the spectral response of the aluminum, with the solar energy distribution, the theoretical solar-weighted optical efficiency of 89% can be determined for the collector reflection response. Further, assuming an expected intercept factor of 0.99 and a receiver conversion efficiency of 90%, results in a 79% solar-to-thermal efficiency. The measured collection efficiency of 72% achieved by the PSU Berks collector during the heat gain tests thus compares favorably with the near ideal 0.79 value of R_{Θ}, or 79% solar-to-thermal conversion.

There are potential improvements that can be made to the FOCUS collector mirrors that could improve optical efficiency and reduce cost. The reflectors used in the current tests were fabricated with each petal elastically formed by stretching the precut flat media

over a mandrel and welding it to a frame to maintain its curvature. Forcing a flat piece of sheet metal into a parabolic shape intrinsically imparts stresses that result in reflector surface slope errors. In addition, the welding process leaves distortions that extend well beyond the domain of the weld. Collectively these effects account for the major portion of the optical losses and departure of the real reflector from that of the ideal reflector surface.

Future improvements in reflector surface manufacturing will reduce slope errors and eliminate the welding distortions. Petals will be fabricated using a stamping process similar to that used in the automotive industry to fabricate body panels. Low temperature adhesives will be used to assemble petals into the collector, eliminating potential welding distortions. These manufacturing processes will improve the intercept factor and the concentration ratio at the focal plane and will in turn allow the aperture of the receiver to be decreased, reducing convection losses. With these and other improved manufacturing and implementation approaches, it is not unrealistic to anticipate solar-to-thermal conversion efficiency for the FOCUS in the range of 74% to 75% or higher.

References

1. World Health Organization, Household air pollution and health, 8 May 2018. https://www.who.int/news-room/fact-sheets/detail/household-air-pollution-and-health
2. United Nations, Background Note on Wood Energy in India. https://www.un.org/esa/forests/wp-content/uploads/2018/05/UNFF13_Background_Note_Wood_Energy_in_IndiaTERI.pdf
3. Measurements conducted at Optical Data Associates
4. Measured using Filmetrics FR10 reflectance meter
5. Measured using a Filmetrics FR10 reflectance meter
6. https://earth.google.com/web/search/40%c2%b0+21%27+51.4%27%27+N+75%c2%b0+58%27+36.3%27%27+W/@40.36420381,-75.97676602,73.86300892a,99.6494462d,35y,0h,0t,0r/data=CigiJgokCUZLYYGjSkRAEfa3qwUzJkRAGcbpIq9i01LAIRwUifVGAVPA